

# MODELLING OF THE MECHANICAL BEHAVIOUR POROUS MATERIALS:

## A NEW APPROACH

F. Cosmi, F. Di Marino

*Dipartimento di Energetica, Università di Trieste, 34127 Trieste, Italy*

### **Abstract.**

A new approach to porous materials modelling is presented. In this model a matrix of cells contains a number of randomly distributed void cells in order to obtain the desired porosity. The system is solved by means of a recent numerical method, the Cell Method. As an application, the Young modulus of four sintered alloys is computed and the simulations show a good agreement with the experimental results reported in literature, depending on the porosity of the sintered powder and the Young modulus of the wrought material. Besides this application, the approach is promising in a wider class of problems, namely all those in which a large number of random distributed heterogeneities or voids is present.

### **1. Introduction.**

The Cell Method (CM) has recently been developed [1, 2]. It is currently being applied to several problems, and it has some advantages over more widely used numerical methods, like FEM.

CM has already been applied to thermal conduction, mechanics of deformable solids, fracture mechanics, and electromagnetic wave propagation [3 - 7]. In all these cases the CM results agree with those obtainable with other widely used numerical methods (FEM and FDTD - Finite Difference in Time Domain), but there is something more to CM.

One of the major drawbacks of FEM is that the method cannot be applied when large variations in gradient are present. This is why FEM models are unsuitable whenever the size of the mesh is not smaller than any typical size involved in the geometry of the sample [8]. This drawback directly stems from the use of a differential formulation of the physical laws involved in the considered phenomenon. On the contrary, CM uses global - integral - variables to derive *directly* a discrete formulation of the physical laws. As a consequence, all functions of position - field functions -

describing variables involved in the constitutive equation do not need to be differentiable. This is a good point whenever the displacement field undergoes large variations, i.e. when the size of the heterogeneities is the same scale of that of the cells.

It must be pointed out that, although CM uses global variables in order to write equilibrium equations, it needs - just as any other method - writing constitutive equations at a local level. However, it is easy to see that CM is deeply different from FEM: in CM no energy functional is computed, no differentiation is needed to minimize it.

## **2. The Cell Method.**

Let us give a brief description of the method for plane elasticity. First of all we can think of the variables involved in any field problem as belonging to one of the following classes:

- *configuration variables* – geometrical and kinematic variables, i.e. displacements, velocities, strain tensor;
- *source variables* – static and dynamic sources of the field, i.e. forces, momenta, stress tensor;
- *energy variables*, from the product of the previous two, which we are not going to use in the following.

Given this classification, we may perform a discretization of a continuum sample by means of two staggered complexes of cells (Fig.1):

- *a Delunay complex*, whose primal cells are associated to configuration variables, defining the connectivity of the nodes;
- *a dual Voronoi complex* with which source variables are correlated, in order to write equilibrium equations.

We may think of the dual cell as an influence region for the node. The equilibrium equations may then be written for each dual cell. In this way equilibrium is established over the entire influence region of the node, collecting the contribution from each primal cell surrounding the node. Only global variables are used, and equilibrium equations are directly derived in a discrete form,

embedding the various contributions from each primal cell surrounding the node in the form of an equilibrium equation.

For an affine (linear plus a constant) approximation of the displacement field over the primal cell, strain components are constant within each cell and can be written as [7]:

$$\begin{Bmatrix} \varepsilon_x \\ \varepsilon_y \\ \gamma_{xy} \end{Bmatrix} = -\frac{1}{2tA_c} \begin{bmatrix} A_{hx} & 0 & A_{ix} & 0 & A_{jx} & 0 \\ 0 & A_{hy} & 0 & A_{iy} & 0 & A_{jy} \\ A_{hy} & A_{hx} & A_{iy} & A_{ix} & A_{jy} & A_{jx} \end{bmatrix} \begin{Bmatrix} u_{hx} \\ u_{hy} \\ u_{ix} \\ u_{iy} \\ u_{jx} \\ u_{jy} \end{Bmatrix} \quad (1)$$

where  $t$  is the thickness of the sample,  $u_{ij}$  denotes the node  $i$  displacement component along the  $j$  axes,  $A_c$  is the area of the primal cell,  $A_i$  represents the area of the primal cell side opposed to node  $i$  and  $A_{ij}$  is the projection of  $A_i$  along the  $j$  axes, as shown in Fig.2.

Equation (1) can be written in a more synthetic form as

$$\{\varepsilon\}_c = [B]_c \{u\}_c \quad (2)$$

Introducing the constitutive matrix of the primal cell,  $[D]_c$ , Hooke law for each primal cell may be written as

$$\{\sigma\}_c = [D]_c \{\varepsilon\}_c = [D]_c [B]_c \{u\}_c \quad (3)$$

where  $\{\sigma\}_c$  collects the stress components.

As already stated, equilibrium equations are written for the dual region, that is the influence region of each node of the primal cell. In order to do so, the surface forces acting on the two sides of the dual polyhedron surrounding each node inside the primal cell must be expressed.

Let us consider the part (two sides) of the dual polyhedron of node  $h$  that falls inside a primal cell  $c$  (Fig.3). The forces acting through these sides will be  $T'_h$  and  $T''_h$ . With reference to Fig.3, it can be seen that

$$T_h = T'_h + T''_h$$

and remembering that stress components are uniform within each cell whenever an affine interpolation of the displacement field is assumed, the surface force  $T_h$  will be given by

$$\begin{Bmatrix} T_{hx} \\ T_{hy} \end{Bmatrix}_c = \frac{1}{2} \begin{bmatrix} A_{hx} & 0 & A_{hy} \\ 0 & A_{hy} & A_{hx} \end{bmatrix} \begin{Bmatrix} \sigma_x \\ \sigma_y \\ \tau_{xy} \end{Bmatrix}_c$$

For the three nodes of the cell

$$\begin{Bmatrix} T_{hx} \\ T_{hy} \\ T_{ix} \\ T_{iy} \\ T_{jx} \\ T_{jy} \end{Bmatrix}_c = \frac{1}{2} \begin{bmatrix} A_{hx} & 0 & A_{hy} \\ 0 & A_{hy} & A_{hx} \\ A_{ix} & 0 & A_{iy} \\ 0 & A_{iy} & A_{ix} \\ A_{jx} & 0 & A_{jy} \\ 0 & A_{jy} & A_{jx} \end{bmatrix} \begin{Bmatrix} \sigma_x \\ \sigma_y \\ \tau_{xy} \end{Bmatrix}_c$$

and, from (2) and (3), for each primal cell  $c$  we obtain

$$\{T\}_c = -tA_c [B]_c^T [D]_c [B]_c \{u\}_c$$

where for this simulation isotropic linear elastic plane stress was assumed.

It is now possible to write the equilibrium condition for each dual cell. We make the following propositions:

- $\tilde{U}_h$  is the dual cell surrounding node  $h$  (Fig. 4);
- $\mathbf{T}_h^c$  is the resultant surface force acting on the two sides of  $\tilde{U}_h$  belonging to cell  $c$ ;
- $\mathbf{T}_h$  is the total force acting on the boundary of  $\tilde{U}_h$  due to all the cells surrounding node  $h$

$$\mathbf{T}_h = \sum_c \mathbf{T}_h^c$$

- $\mathbf{F}_h^c$  is the volume force acting on the part of  $\tilde{U}_h$  belonging to cell  $c$ ;
- $\mathbf{F}_h$  is the resultant volume force acting on  $\tilde{U}_h$

$$\mathbf{F}_h = \sum_c \mathbf{F}_h^c$$

Equilibrium for each node  $h$  can be expressed by the set of  $n$  equations (where  $n$  is the number of nodes)

$$\mathbf{T}_h + \mathbf{F}_h = 0$$

If cell  $c$  rests on the boundary of the sample (Fig.5),

•  $\mathbf{B}_h$  is the resultant of the external forces acting on  $\tilde{U}_h$  through the boundary cells

and equilibrium equations become

$$\mathbf{T}_h + \mathbf{F}_h + \mathbf{B}_h = 0$$

that is a set of  $2n$  linear equations in the  $2n$  unknowns  $u_{ix}, u_{iy}$  ( $i=1, \dots, n$ ), which can be solved with the usual methods.

### 3. Sintered alloys compression simulation.

Mechanical properties of sintered alloys are known to depend strongly on residual porosity. In the proposed model, the primal cells can be of two kinds: ferrous and voids. Voids are randomly distributed among the ferrous cells in order to obtain the desired porosity. A compression test is then simulated, and the estimated value of Young modulus computed.

As already stated, the equilibrium equations have been directly derived in a discrete form, and can therefore embed discontinuities of the constitutive matrix  $[D]$  from one primal cell to the adjacent.

It has already been mentioned that at this stage only linear elastic plane stress has been considered within each primal cell. The model at present is limited to compression. In fact, small non-linearities in strain/stress behavior below the macroscopic yield occur in experimental tension tests of sintered alloys. This progressive damage accumulation at the moment has not been taken into account by the model.

The method has been implemented in Fortran. Trials have been run imposing a simulated compression test (actually a negative relative displacement) on bars with various densities of random distributed voids.

The primal mesh always had 5340 cells. The prismatic specimen modeled was 10x38 mm. Fig. 6 shows the primal and dual meshes used.

The simulation results are compared with the experimental values reported for compression tests in Bertini et al. [9]. Five simulations have been performed for each alloy, which is the same number of

compression tests performed by the authors of [9]. Four different ferrous sintered alloys have been considered.

The size of the primal cells in the simulations was chosen as to compare with the size of the heterogeneities that are usually found in sintered materials.

Porosity changed slightly from one simulation to the other, while porosity distribution was random.

In the following:

$E_0$  = Young modulus of wrought material,

$E_S$  = experimental compressive Young modulus,

$E_{CM}$  = computed compressive Young modulus.

Each of the simulated materials A1 and A2 is shown in Fig. 7 and 8, respectively. In order to improve readability void cells are printed in black, while ferrous ones are shown white. Average results for material A1 and A2 are shown in Table 1 and Table 2 respectively. Each of the simulated materials B1 and B2 is shown in Fig. 9 and 10, while the average results for them are shown in Table 3 and Table 4, respectively.

Details of the simulations results are given in Table 5 for materials A1 and A2 and in Table 6 for materials B1 and B2. It can be seen that, although a general trend is present (increasing porosity will decrease apparent Young modulus), porosity alone is not sufficient to account for all the variations: different distributions of voids in the matrix lead to different “structures”, porosity being equal (see results from simulations 1 and 4 for material A2). On the other sides, different porosity distributions will lead to the same result, although porosity has changed (see simulations 2 and 5 for material B1).

Graphs showing the dependency of  $E_{CM}$  on porosity of materials A1 and A2 are shown in Fig. 11, while for materials B1 and B2 are shown in Fig. 12, which again show the general trend and the previously discussed scatter.

#### **4. Conclusions.**

Although at the moment the model assumes a simple linear constitutive law for the filled cells and linear interpolation functions for the displacement field, the obtained results are very promising.

Deviation between experimental and simulation results was never greater than 10%, which is within the usual range of variability for such materials.

Higher order interpolation for CM has already been implemented [7,10], but it would be more important for the purpose of the present research to introduce rheological behaviors other than the elastic one. An elastic-plastic incremental model has been developed and discussed in [11] and will be applied to sintered materials mechanical behavior modeling.

### **Acknowledgements**

The authors wish to thank prof. Enzo Tonti, University of Trieste, whom the Cell Method is due, for his precious advice. Thanks are also directed to Fabio Miani, University of Udine, for helpful discussions.

### **Bibliography**

- [1] Tonti E. *Formulazione finita delle equazioni di campo: Il Metodo delle Celle*, Atti del XIII Convegno Italiano di Meccanica Computazionale, Brescia, Italy, 2000
- [2] Tonti E. *A Direct Discrete Formulation of Field Laws: The Cell Method*, Computer Modeling in Engineering & Sciences, vol.2, n.2, 2001
- [3] Marrone, M. *Computational Aspects of Cell Method in Electrodynamics*, J. Electromagnetic Waves and Applications, Vol.15, N.3
- [4] Tonti, E. *A Finite Formulation for the Wave Equation*, Journal of Computational Acoustics, in printing.
- [5] Nappi, A., Rajgelj, S., Zaccaria, D., *A Discrete Formulation Applied to Crack Growth Problems*, Proc. Meso Mechanics, 2000 Conference, Xi'an, China.
- [6] Cosmi F., Di Marino F., *A New Approach to Sintered Alloys Mechanical Behavior Modeling*, Proc. of 17<sup>th</sup> Danubia Adria Symposium on Experimental Methods in Solid Mechanics, Prague, Czech Republic, 2000

- [7] Cosmi F., *Numerical Solution of Plane Elasticity Problems with the Cell Method*, Computer Modeling in Engineering & Sciences, vol.2, n.2, 2001
- [8] Roux,S. *Continuum and Discrete Description of Elasticity*, in Statistical Models for the Fracture of Disordered Media, H.J. Herrmann and S. Roux (editors) Elsevier Science Publishers B.V. (North Holland), 1990, pp. 109-113.
- [9] Bertini,L., Fontanari,V., Straffellini,G., *Tensile and Bending Behaviour of sintered alloys: Experimental results and Modelling*, Jour. of Engineering Materials and Technology, July 1998, vol.120, pp. 248-255.
- [10] Cosmi,F., *Applicazione del metodo delle celle con approssimazione quadratica*, Atti del XXIX Convegno Nazionale AIAS, Lucca, September 6-9, 2000.
- [11] Cosmi,F., *Elasto-plasticità con il metodo delle celle*, Atti del XXX Convegno Nazionale AIAS, Alghero, September 12-15, 2001.

FIGURES

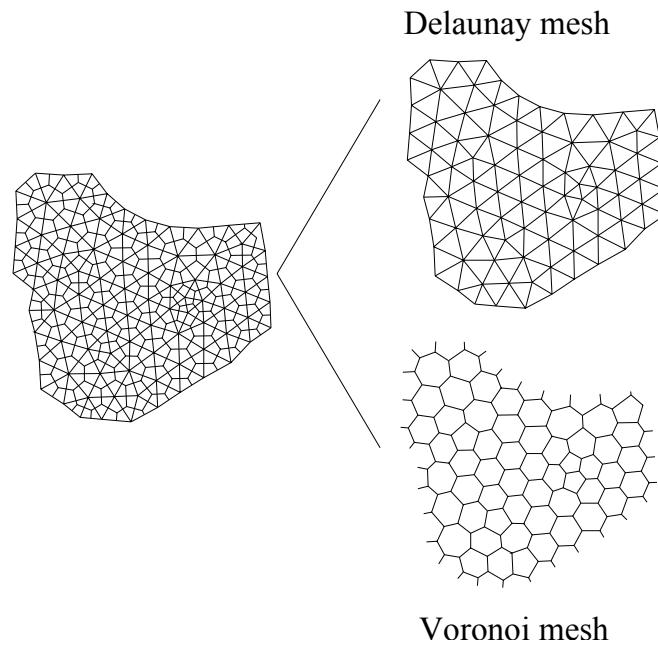


Figure 1: Primal and dual cells complexes

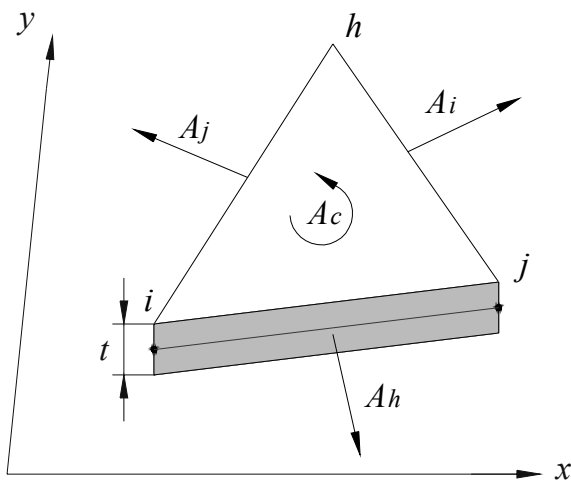


Figure 2: Geometrical quantities

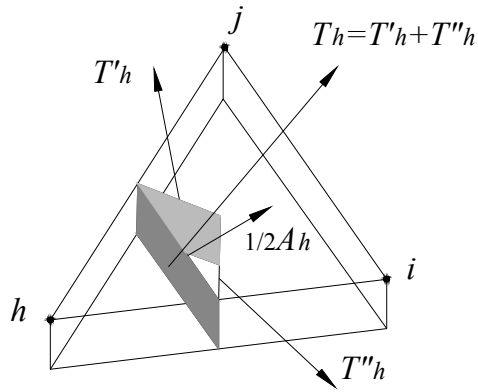


Figure 3: Forces through the sides of the dual cell of node  $h$ .

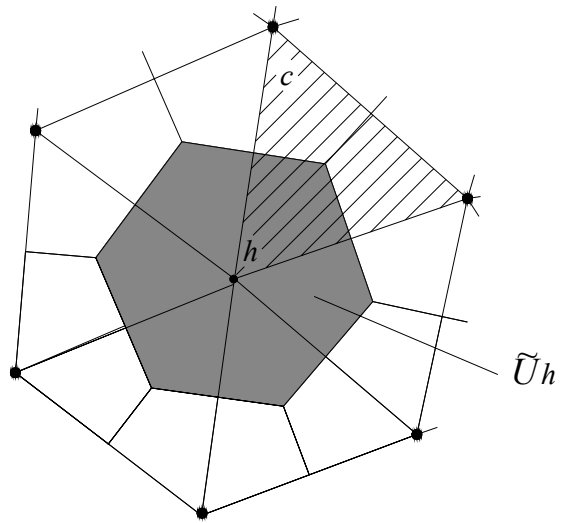


Figure 4: Dual cell of node  $h$ .

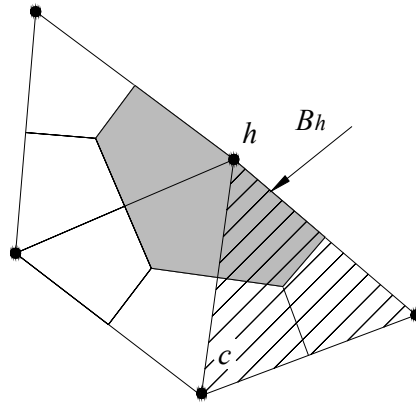


Figure 5: Boundary dual cell.

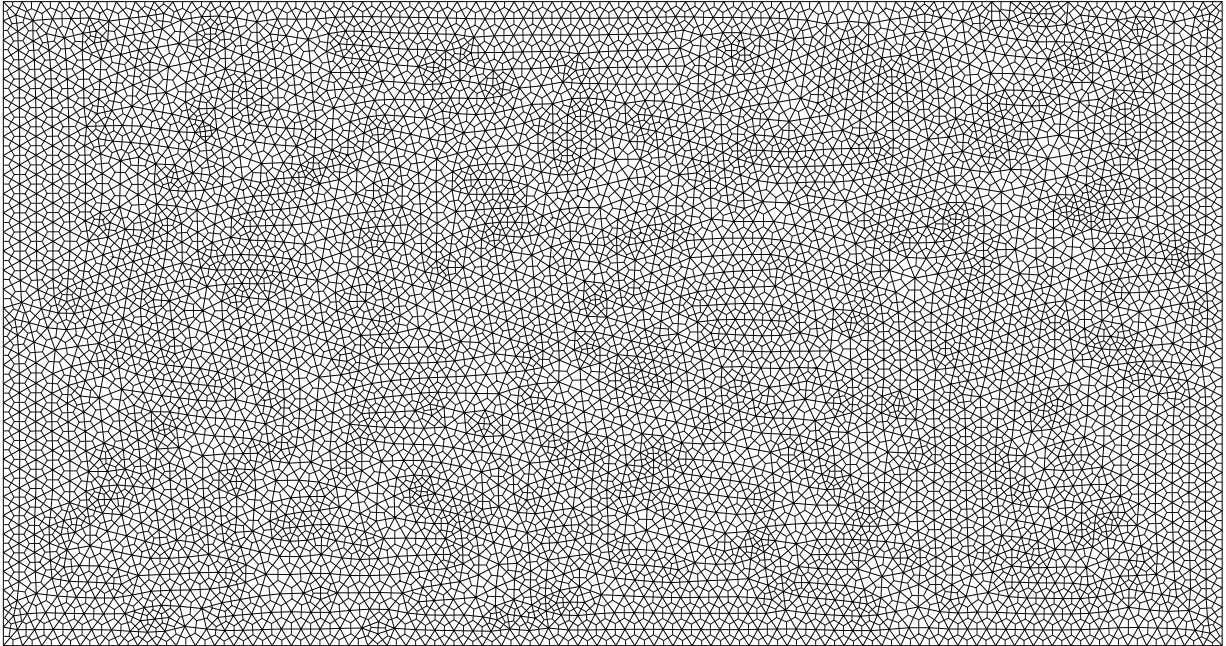


Figure 6: The Delunay and Voronoi meshes used in the simulations

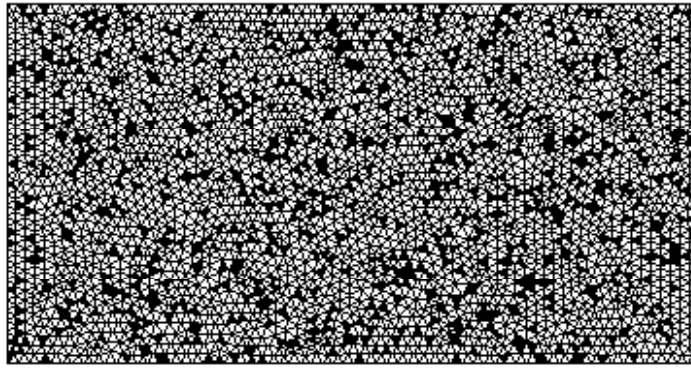


Figure 7: Material A1

Table 1

Material	A1
Commercial powder	NC100.24
$E_0$	207 GPa
Porosity content	13.4 %
$E_S$	150 GPa
Average porosity of the model	13.25 %
$E_{CM}$	138 GPa
Deviation	8 %

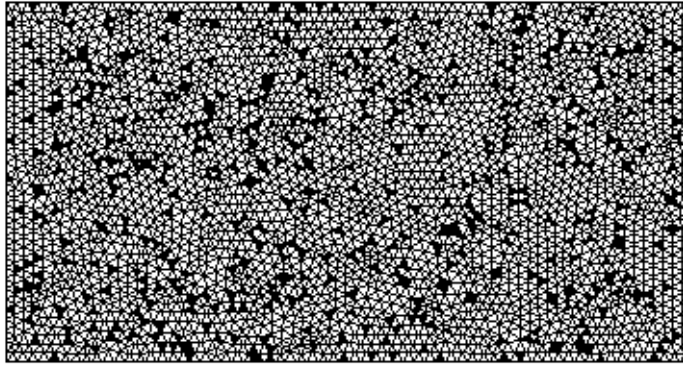


Figure 8 - Material A2

Table 2

Material	A2
Commercial powder	NC100.24
$E_0$	207 GPa
Porosity content	9.8 %
$E_S$	168 GPa
Average porosity of the model	10.1 %
$E_{CM}$	155 GPa
Deviation	7.7 %

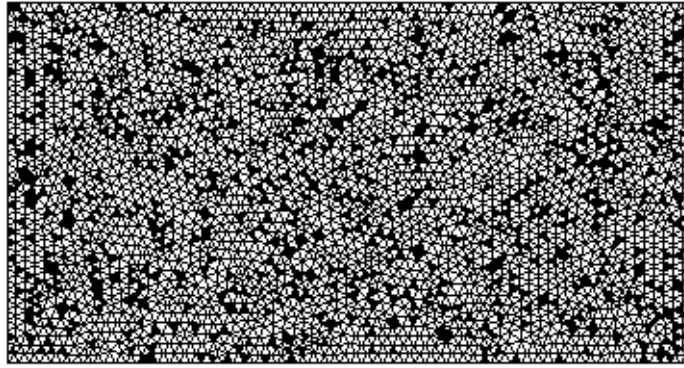


Figure 9 - Material B1

Table 3

Material	B1
Commercial powder	AISI316L
$E_0$	197 GPa
Porosity content	14.5 %
$E_S$	140 GPa
Average porosity of the model	14.34 %
$E_{CM}$	125 GPa
Deviation	10 %

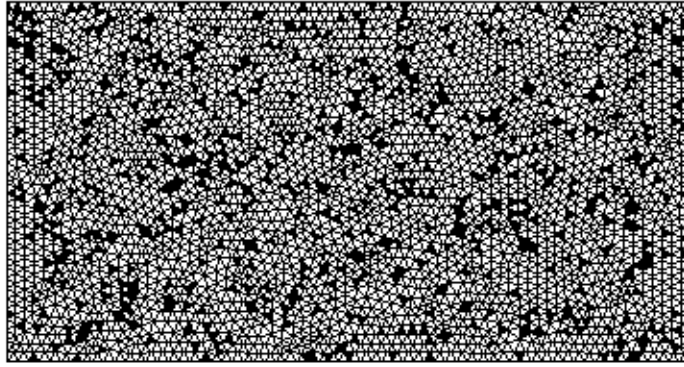


Figure 10 - Material B2

Table 4

Material	B2
Commercial powder	AISI316L
$E_0$	197 GPa
Porosity content	11.9 %
$E_S$	150 GPa
Average porosity of the model	12.04 %
$E_{CM}$	138 GPa
Deviation	8 %

Table 5

	Material			
	A1		A2	
Simulation	Porosity	$E_{CM}$ (Gpa)	Porosity	$E_{CM}$ (Gpa)
1	12.8	143	9.7	155
2	13.9	138	10.6	154
3	13.6	128	10	156
4	13.4	137	9.7	158
5	12.6	142	10.4	152

Table 6

	Material			
	B1		B2	
Simulation	Porosity	$E_{CM}$ (Gpa)	Porosity	$E_{CM}$ (Gpa)
1	14.1	126	12.2	135
2	14.4	125	12.5	133
3	14.3	124	11.6	140
4	14.3	124	11.8	138
5	14.6	125	12.1	143

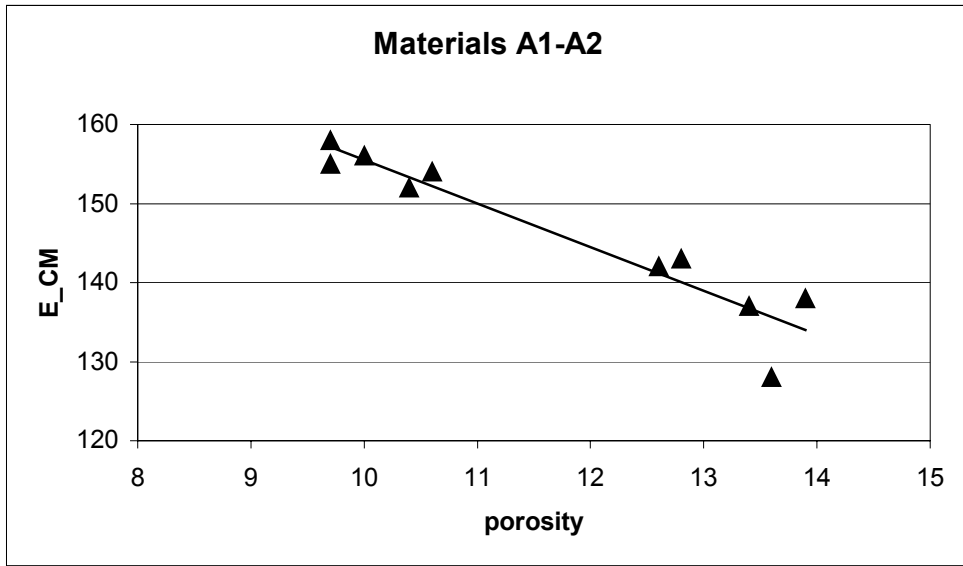


Figure 11: Dependency of  $E_{CM}$  on porosity of materials A1 and A2.

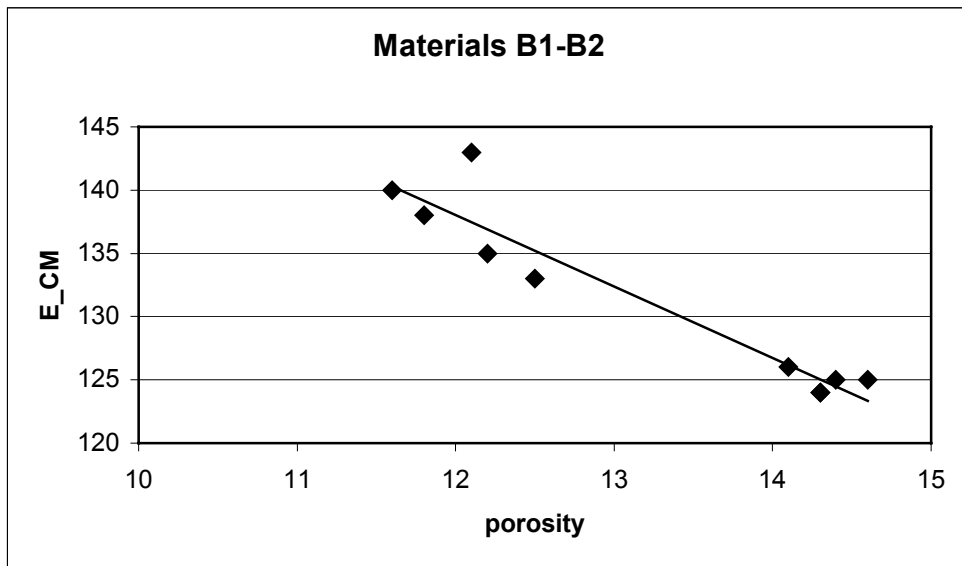


Figure 12: Dependency of  $E_{CM}$  on porosity of materials B1 and B2